Chapter 2
Harmonic Power Flow Calculation for High-Speed Railway Traction Power Supply System

Bin Wang, Xu dong Han, Shi bin Gao, Wen Huang and Xiao feng Jiang

Abstract This paper describes a harmonic analysis model for CRH2 EMU (Electric Multiple Unit) and provides a harmonic power flow algorithm for its traction power supply system. This algorithm gives full consideration to coupling influence between the traction networks (harmonic voltage), and the fundamental wave results are used as the final convergence condition, aiming to determine modulation characteristics and harmonic current characteristics of SPWM converter for EMU based on results of harmonic power flow, and to calculate harmonic power flow and to update fundamental power of harmonic source for fundamental power flow calculation. Analysis of harmonic power flow with single harmonic source and multi-harmonic sources shows that the algorithm is applicable to traction power supply system of high-speed rail with single harmonic source, multi-harmonic sources, and background harmonic.

Keywords Locomotive and network coupling system · Harmonic power flow · EMU harmonic model · Harmonic coupling admittance matrix

2.1 Introduction

Electrified railway is always one of the main harmonic sources of electric power system; and high-speed railway directly accesses HV electric power system of 220 kV or higher voltage. For the purpose of effectively calculating and analyzing distribution characteristics of harmonic in traction network and its permeability characteristics toward electric power system, harmonic power flow of traction power supply system needs to be analyzed and calculated [1, 2].

Firstly, harmonic characteristics of locomotive as well as the coupling link between its harmonic voltage and harmonic current need to be established, so as to

B. Wang (✉) · X. d. Han · S. b. Gao · W. Huang · X. f. Jiang
School of Electrical Engineering, Southwest Jiaotong University, Chengdu, Sichuan Province, China
e-mail: bwang@swjtu.edu.cn

L. Jia et al. (eds.), *Proceedings of the 2013 International Conference on Electrical and Information Technologies for Rail Transportation (EITRT2013)-Volume I*, Lecture Notes in Electrical Engineering 287, DOI: 10.1007/978-3-642-53778-3_2,

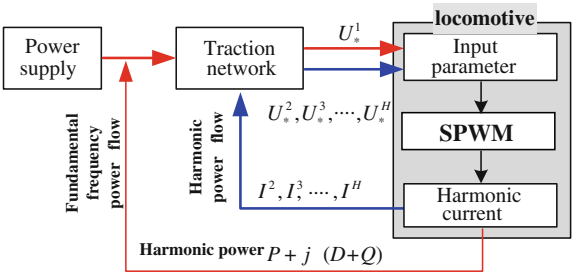

Fig. 2.1 Basic schematic of harmonic power flow calculation

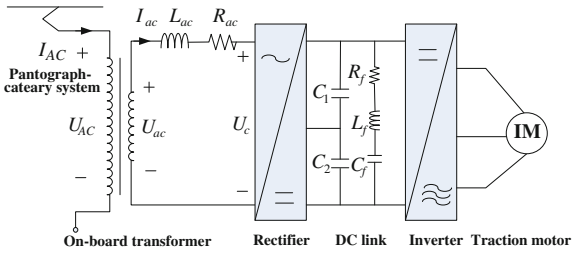

Fig. 2.2 Schematic diagram of traction-drive system

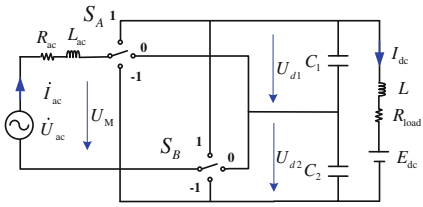

Fig. 2.3 Three-level rectifier equivalent circuit

propose a harmonic power flow algorithm suitable for traction power supply system of high-speed railway: embed harmonic power flow into fundamental power flow and correct load power output by using harmonic power of harmonic source; update harmonic current and harmonic power based on calculated results of fundamental power flow and harmonic power flow, and finally calculate distribution of network harmonic voltage based on harmonic power flow and calculate distribution of network fundamental voltage based on fundamental power flow. The calculation framework is shown in the following Fig. 2.1.

2.2 EMU Harmonic Model

2.2.1 EMU Simulation Model

Traction-drive system of high-speed train mainly consists of on-board transformer, SPWM converter, DC link (voltage regulation and filtration), SVPWM inverter, and three-phase AC traction motor is as shown in Fig. 2.2.

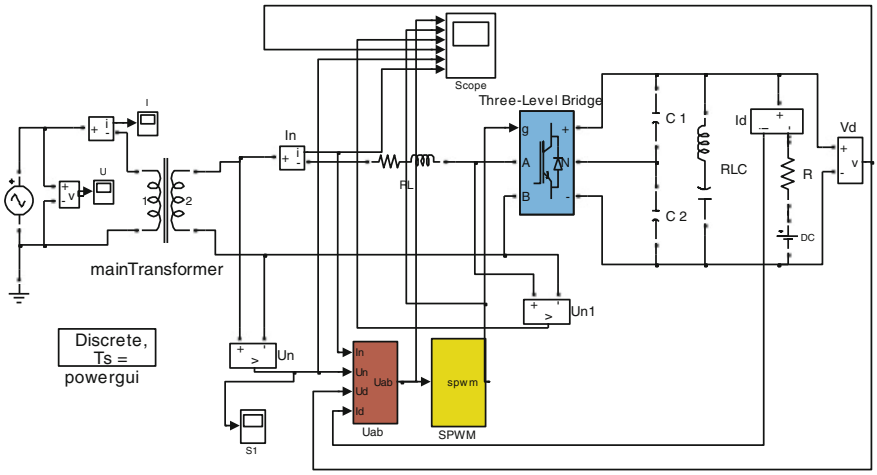

Fig. 2.4 CRH2 traction-drive system simulation model

If power switching device of rectifier is regarded as ideal element, the main circuit of Electric Multiple Unit (EMU) can be equivalent, as shown in Fig. 2.3.

According to the actual parameters [3–5], the establishment of CRH2-type EMU simulation model is shown in Fig. 2.4.

2.2.2 Analysis of EMU Harmonic Characteristics

If power switching device of rectifier is regarded as ideal element, the results of simulation analysis by this model are shown in Fig. 2.5a.

Further more, power supply system with background harmonic as shown in Table 2.1 is taken for harmonic spectrum analysis of EMU. Comparison between Fig. 2.5b, c shows that harmonic current spectrum of EMU is changed after addition of background harmonic; as a result, total harmonic distortion of current (ITHD) increases to 3.48 % from 3.09 %.

After pulsing fundamental voltage, the 1–120th harmonic voltage with amplitude of 0.01 pu (fundamental voltage is the rated voltage) and phase angle of 0° is compared with single action of fundamental voltage and a bar chart as shown in Fig. 2.6 is obtained. It indicates that: ① Fundamental voltage has a great impact on harmonic current, such as the 40–60th (2MR ± 10) and the 100–120th (4MR ± 10). ② Harmonic voltage has a slight impact on fundamental current. ③ The diagonal element shows that the *h*th harmonic voltage has great impact on the *h*th harmonic current, and the influence of fundamental voltage on fundamental current reaches 100 %. Influence of the 3rd harmonic voltage on the 3rd harmonic current can reach 150 % and others show a decline trend. This is consistent with

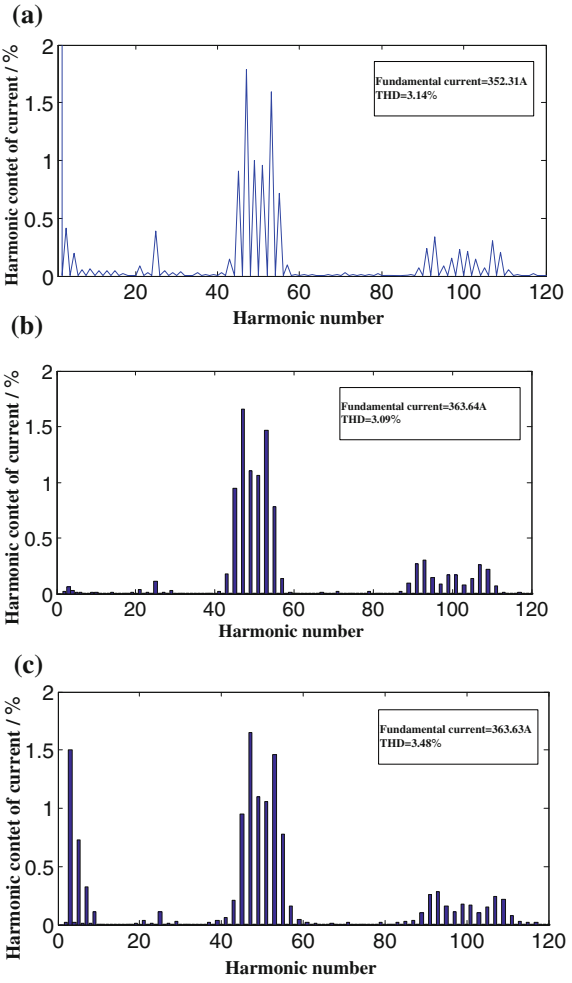

Fig. 2.5 Harmonic analysis of EMU. **a** Simulation analysis results by Simulink, **b** EMU current spectrum under ideal circumstance, **c** EMU current spectrum with background harmonic

Table 2.1 Parameter of background harmonics

Harmonic number	Fundamental wave	3rd	5th	7th	9th
Amplitude / %	100	1.0	0.8	0.5	0.2
Phase angle / °	0	20	−70	80	−85

conclusion drawn from Fig. 2.6(c). ④ Harmonic admittance for different orders is different. Therefore, separate consideration is required for establishment of harmonic source admittance, which is described hereinafter.

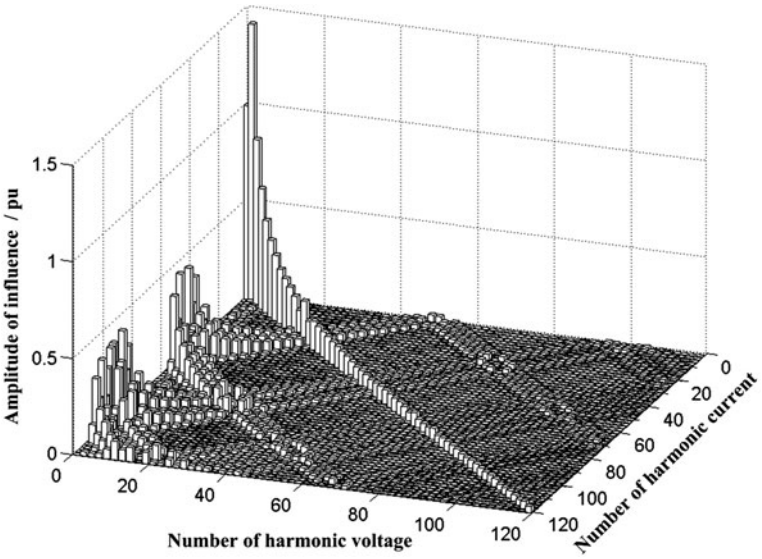

Fig. 2.6 Harmonic coupling admittance matrix

2.3 Harmonic Model of Traction Power Supply System

2.3.1 Schematic Diagram of Traction Power Supply System

The traction power supply system provides EMU with power from three-phase power grid through traction transformer and OCS, as shown in Fig. 2.7.

2.3.2 Harmonic Model of Traction Transformer

Traction transformers of V/v connection are widely used in high-speed railway, as shown in Fig. 2.8.

According to the circuit diagram shown in Fig. 2.8b, node admittance matrix of Vv transformer can be obtained:

$$Y_{\mathrm{TR}} = \frac{1}{k^2 Z_2}\begin{bmatrix} 1 & -1 & -k & k \\ -1 & 1 & k & -k \\ k & -k & -k^2 & k^2 \\ -k & k & k^2 & -k^2 \end{bmatrix} \tag{2.1}$$

where Z_2 is equivalent impedance on secondary side of traction transformer and $Z_2 = \sqrt{h}R_2 + \mathrm{j}hX_2$; k is transformer turns ratio and $k = 220$ kV/55 kV.

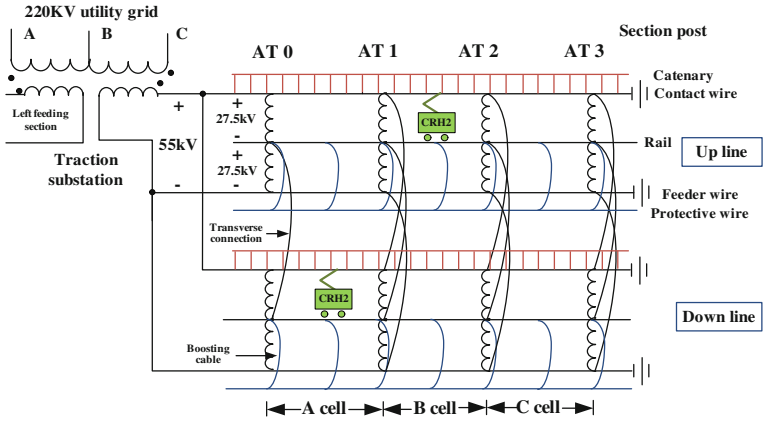

Fig. 2.7 Typical high-speed railway traction power supply system

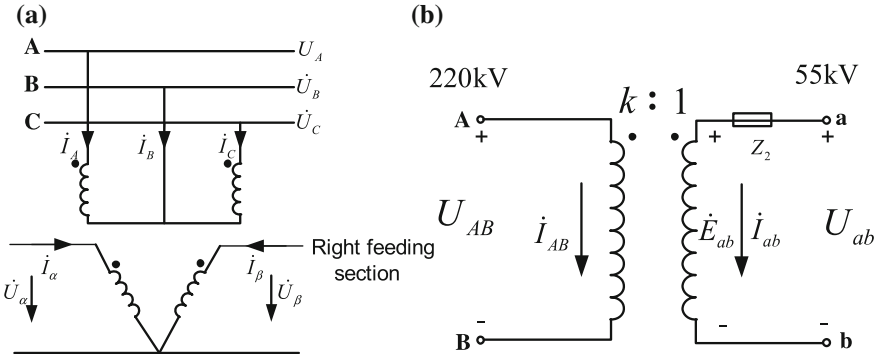

Fig. 2.8 Vv traction transformer circuit model. **a** Vv transformer. **b** Right feeding section

2.3.3 Harmonic Model of Traction Network

All-parallel AT power supply mode is widely employed for high-speed railway. The traction network is decomposed as per the unit of 1 km for modeling while full consideration is given to characteristics of traction network distribution parameters. Chain circuit theory is used to establish the equivalent model of the traction network [6] and an equivalent chain circuit model is obtained, as shown in Fig. 2.9.

Combing with Fig. 2.9, harmonic node admittance matrix of the system is obtained and shown as below:

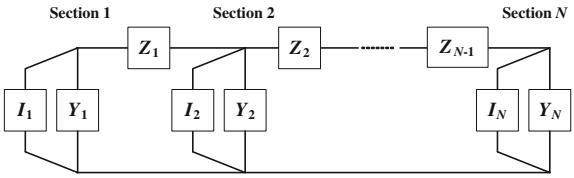

Fig. 2.9 Traction network chain circuit model

$$\boldsymbol{Y}=\begin{bmatrix} \boldsymbol{Y}_1+\boldsymbol{Z}_1^{-1} & -\boldsymbol{Z}_1^{-1} & & & \\ -\boldsymbol{Z}_1^{-1} & \boldsymbol{Z}_1^{-1}+\boldsymbol{Y}_2+\boldsymbol{Z}_2^{-1} & & & \\ & \ddots & \ddots & & \\ & & & \boldsymbol{Z}_{N-2}^{-1}+\boldsymbol{Y}_{N-1}+\boldsymbol{Z}_{N-1}^{-1} & -\boldsymbol{Z}_{N-1}^{-1} \\ & & & -\boldsymbol{Z}_{N-1}^{-1} & \boldsymbol{Z}_{N-1}^{-1}+\boldsymbol{Y}_N \end{bmatrix} \tag{2.2}$$

2.3.4 Admittance Model of Harmonic Source

Certain approximate linear relationship exists between harmonic voltage and harmonic current at a certain frequency [7, 8], i.e.,

$$Y_h = \dot{I}_h/\dot{U}_h \tag{2.3}$$

For linear load, if the effective value of its bus bar voltage is U_L, absorbed active power is P_L, and reactive power is Q_L, its equivalent fundamental power can be equivalent to parallel admittance form in frequency domain, as shown below:

$$Y_\mathrm{L}=(hQ_\mathrm{L}+\mathrm{j}P_\mathrm{L})/hU_\mathrm{L}^2 \tag{2.4}$$

2.4 Harmonic Power Flow Algorithm in Case of Locomotive and Network Coupling

2.4.1 Calculation of Fundamental Power Flow by Using N-R Method

For calculation of fundamental power flow by using N-R method, impact of harmonic power shall be taken into account [9]. According to analysis in Sect. 2.2, harmonic power of harmonic source can be obtained:

$$\begin{aligned} S_i &= \sqrt{\sum_{h=1}^{H}\left(\dot{U}_i^h\right)^2}\cdot\sqrt{\sum_{h=1}^{H}\left(\dot{I}_i^h\right)^2} \\ P_i &= \sum_{h=1}^{H}\mathrm{Re}\left(\dot{U}_i^h\dot{I}_i^h\right) \\ Q_i &= \sqrt{(S_i)^2-(P_i)^2} \end{aligned} \tag{2.5}$$

Node at the locomotive side is regarded as PQ node and the PQ node is corrected according to Formula (2.1), as shown below:

$$\begin{aligned} \Delta P_i &= P_i^{SP} - P_i \\ \Delta Q_i &= Q_i^{SP} - Q_i \end{aligned} \tag{2.6}$$

2.4.2 Harmonic Power Flow Algorithm

Through above analysis, output harmonic current of harmonic source can be finally obtained by using the harmonic source model. For the hth harmonic, node voltage equation of the system is:

$$U_h = \boldsymbol{Y}_h^{-1} I_h \tag{2.7}$$

where $\boldsymbol{Y}_h$ is system harmonic admittance matrix of the hth harmonic; $I_h = \begin{bmatrix} I_1^h & I_2^h & \ldots & I_n^h \end{bmatrix}^{\mathrm{T}}$ is the hth injected harmonic current vector of system node; and $U_h = \begin{bmatrix} U_1^h & U_2^h & \ldots & U_n^h \end{bmatrix}^{\mathrm{T}}$ is the hth harmonic voltage vector of system node.

However, it is required to convert the system background harmonic voltage $\dot{U}_h$ to injected harmonic current. Considering that the impedance of the capacitance system added $Z_\mathrm{s} = R_\mathrm{s} + \mathrm{j}hX_\mathrm{s}$, its injected harmonic current is:

$$\dot{I}_h = \dot{U}_h / Z_\mathrm{s} \tag{2.8}$$

Harmonic power flow is calculated combining with Formula (2.7).

2.4.3 Harmonic Power Flow Calculation Procedure

Basic ideas about harmonic power flow proposed in this paper are shown in Fig. 2.10, i.e, deviation of fundamental voltage at each node is used as the measurement index of iteration. Formula for iterative error calculation is shown as below:

$$\varepsilon = \sum_{i=1}^{n}\left\|\dot{U}_i^{(k)} - \dot{U}_i^{(k-1)}\right\| \le 1\,\mathrm{V} \tag{2.9}$$

where i is system node number and $i = 1, 2, 3, \ldots, n$; k is iteration number.

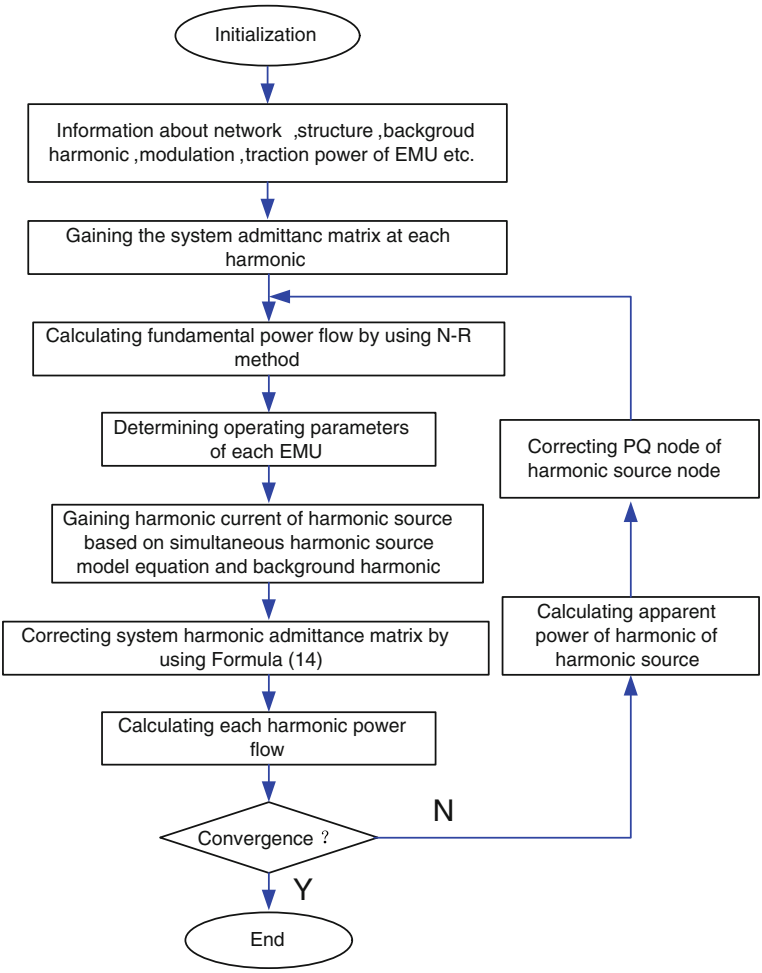

Fig. 2.10 Block diagram for HPF calculation

2.5 Analysis of Calculation Examples

2.5.1 Calculated Power Flow of Single Locomotive

Parameters of calculation examples are relevant parameters described in Ref. [10] (Fig. 2.11).

Harmonic voltage distortion of different positions on the up-track OCS is shown in Figs. 2.12 and 2.13. Harmonic voltage distortion near the 50th and the 100th harmonics is centralized. As a whole, it is the same with locomotive current

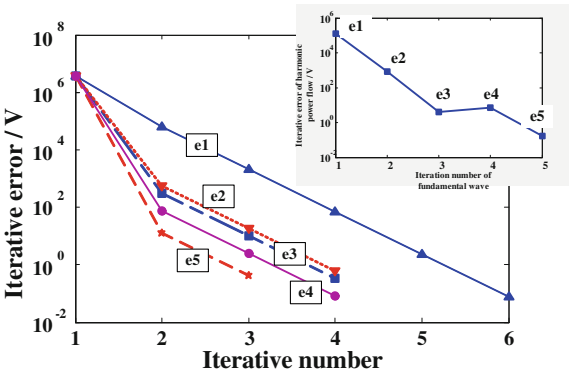

Fig. 2.11 Iteration results

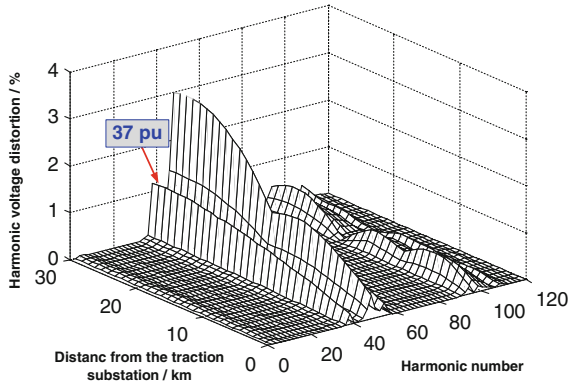

Fig. 2.12 Harmonic distortion of up-track OCS voltage

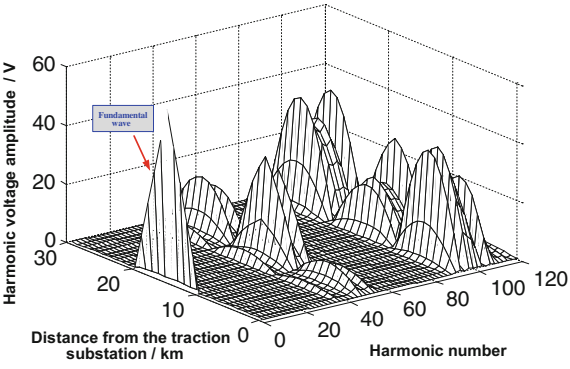

Fig. 2.13 Spectrum analysis of rail voltage

spectrum trend shown in Fig. 2.5. Besides, it is worth noting that the 37th harmonic voltage distortion is around 1 %. Typical locomotive spectrum is obviously amplified.

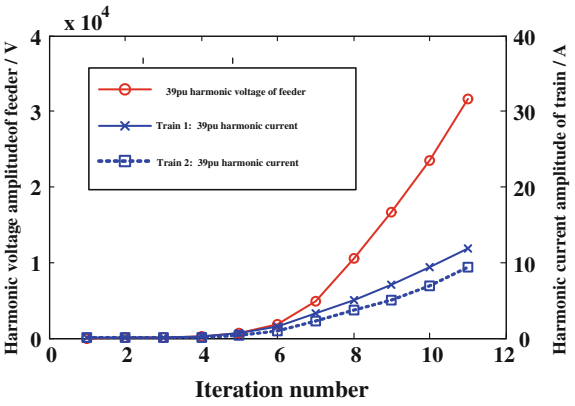

Fig. 2.14 Trent chart of 39 pu harmonic current and voltage

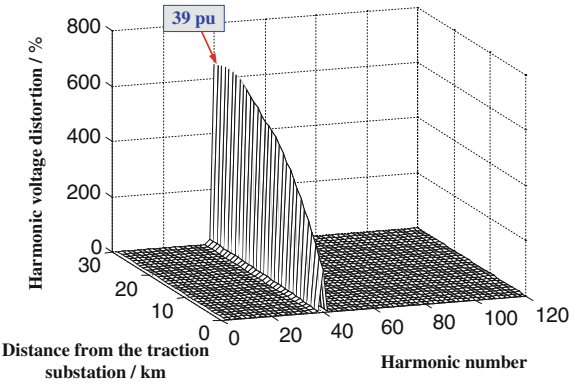

Fig. 2.15 Harmonic distortion of up-track OCS voltage

2.5.2 *Calculated Power Flow of Multiple Locomotives*

This example has two locomotives in the same feeding section. According to Fig. 2.14, harmonic is not converged during harmonic power flow calculation. Thus, harmonic resonance occurs. Conclusion drawn from this calculation example is consistent with References [11, 10, 12]. Accordingly, harmonic power flow calculation in this paper is demonstrated to be reasonable. At the moment, with harmonic distortion of OCS voltage and rail voltage, the 39th harmonic resonance has occurred in the system, as shown in Figs. 2.15 and 2.16. As shown in Fig. 2.16, harmonic voltage of rail is far more than its fundamental voltage when resonance is likely to occur, which is also a great hazard.

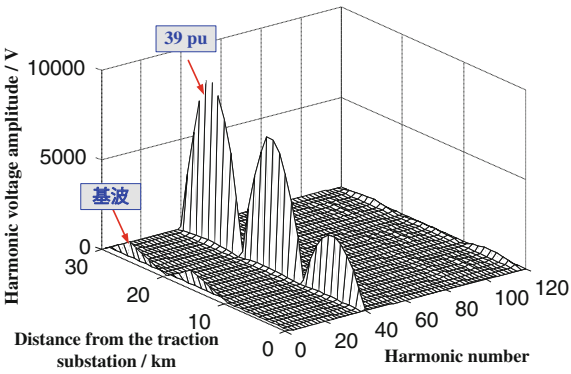

Fig. 2.16 Spectrum analysis of rail voltage

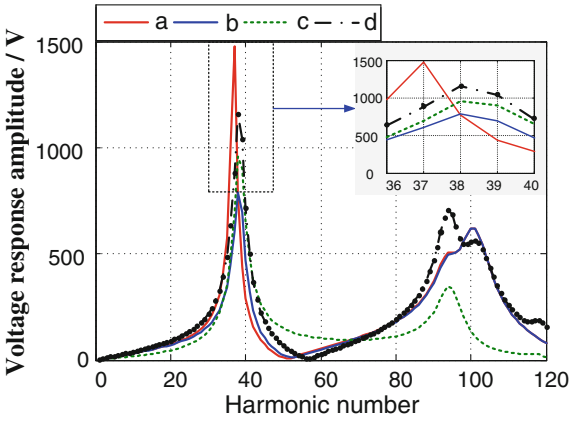

Fig. 2.17 Driving-point impedance of train node

2.6 Discussion

Comparison between calculation example 1 and 2 shows that during operation of a single train, the 37th harmonic is amplified to a certain extent, but converged near 1 %. However, the 39th harmonic in calculation example 2 is not converged. This is because that mutual influence and excitation exist between parameters of the two EMUs; as a result, the 39th harmonic oscillates and cannot be converged. Figure 2.17 shows impedance amplitude of drive point calculated through 2 calculation examples under 4 different circumstances: (a) for calculation example 1, locomotive emits harmonic current and voltage response occurs on the locomotive side; (b) for calculation example 2, locomotive 1 emits harmonic current and locomotive 1 occurs voltage response; (c) for calculation example 2, locomotive 1

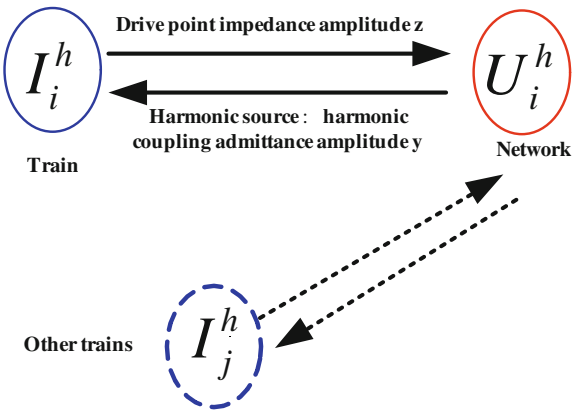

Fig. 2.18 The interaction between harmonic catenary and train in the *h*th harmonic

emits harmonic current and locomotive 2 occurs voltage response; (d) for calculation example 2, locomotive 2 emits harmonic current and locomotive 2 occurs voltage response. Large values occur at the 37th harmonic in calculation example 1 and the 38th and 39th harmonics in calculation example 2. According to current spectrum of train shown in Fig. 2.5, the 36th–38th harmonic current is nearly 0; besides, the two trains are subject to mutual influence and mutual excitation during modulating wave adjustment. As a result, the 39th harmonic resonance occurs in calculation example 2.

According to Fig. 2.18, mutual transformation relationship between the *h*th harmonic voltage and the *h*th harmonic current can be explained. Drive-point impedance z is fixed under the *h*th harmonic; however, admittance value y is changed under harmonic coupling. If the sum of z and y is larger than 1 during all iteration, the iteration is divergent; on the contrary, the iteration is easy to be converged. When the iteration is divergent, it can be considered that the *h*th harmonic resonance occurs. Harmonic resonance is formed due to severe distortion of harmonic voltage of the electric network at certain frequency caused by harmonic current; furthermore, distortion of harmonic voltage will worsen the performance characteristics of the harmonic source and further increase the distortion of harmonic current. Thus, a "positive feedback" process is formed. According to the above analysis, harmonic resonance shall satisfy following conditions:

① Parameters of the electric network (drive-point impedance) match with those of harmonic source impedance (harmonic coupling admittance); ② the harmonic source can generate enough harmonic current and harmonic power at the frequency; ③ the harmonic source is of voltage type rather than stereotype (such as constant current source).In case all above conditions are satisfied, convergence will not occur during harmonic power flow calculation.

2.7 Conclusion

Following conclusions are obtained after analysis of and discussion about harmonic power flow calculation examples for single locomotive and two locomotives:

1. Real modulation process of CRH2 EMU can be simulated by using 2D model. Harmonic model of the EMU gives full consideration to the influence mechanism of harmonic voltage on the AC side on modulating wave and harmonic current.
2. For harmonic power flow, resonance phenomenon usually occurs due to network parameter matching and mutual excitation of harmonic voltage and current; as a result, the iteration cannot be converged. For resonance, three conditions, i.e., parameter matching, harmonic excitation and automatic adjustment, shall be satisfied.
3. Resonance phenomenon cannot be avoided during harmonic power flow iteration. Algorithms in this paper accurately reflect such phenomenon and can be used as references for analysis and governance of harmonic resonance of traction power supply system.

Acknowledgments This work is supported by National Natural Science Foundation of China (No. 51177139); High-speed Rail Joint Fund Key Projects of Basic research (No. U1134205).

References

1. He Z, Hu H, Fang L et al (2011) Research on the harmonic in high-speed railway traction power supply system and its transmission characteristic. Proc CSEE 31(16):55–62 (in Chinese)
2. Chang GW, Lin H-W, Chen S-K (2004) Modeling Characteristics of harmonic currents generated by high-speed railway traction drive converters. IEEE Trans Power Deliv 19(2):766–773
3. Song WS, Xiao FY, WANG LJ et al (2007) Research and simulation on three level 4 quadrant converter based on SPWM modulation. Electr Drive Locomot 4:22–25 (in Chinese)
4. Chen QM, Li YE, Cheng YM et al (2010) Modeling and simulation of vector control system of alternating current motor based on Matlab/Simulink. East China Electr Power 38(5):0740–0744 (in Chinese)
5. Feng JH, Wang J, Li JH (2012) Integrated simulation platform of high-speed train traction drive system. J China Railw Soc 34(2):21–26 (in Chinese)
6. Mingli Wu (2010) Uniform chain model for traction network of electric railways. Proc PSEE 30(28):52–58 (in Chinese)
7. Sun Y, Wang X, Yin Z (2012) Non-iterative harmonic power flow analysis for power systems with multiple harmonic sources. Proc CSEE 32(7):83–90
8. Zhao Y, Zhang T, Li J et al (2002) A new simplified harmonic source model for harmonic analysis and mitigation. Proc CSEE 22(4):46–50 (in Chinese)
9. Arrillaga J, Washton NR (2003) Power system harmonics, 2nd edn. Wiley, London

10. He Z, Hu H, Fang L et al (2011) Research on the harmonic in high-speed railway traction power supply system and its transmission characteristic. Proc CSEE 31(16):55–62 (in Chinese)
11. Guo L, Li Q, Liu W et al (2009) Simulation analysis of dynamic characteristics of harmonics for high-speed locomotive running at rated power. J Southwest Jiaotong Univ 55(6):835–840
12. Hanmin L, Changmu L, Jang G et al (2006) Harmonic analysis of the korean high-speed railway using the eight-port representation model. IEEE Trans Power Deliv 21(2):979–986

http://www.springer.com/978-3-642-53777-6

Proceedings of the 2013 International Conference on Electrical and Information Technologies for Rail Transportation (EITRT2013)-Volume I

Jia, L.; Liu, Z.; Qin, Y.; Zhao, M.; Diao, L. (Eds.)

2014, XV, 652 p. 350 illus., Hardcover
ISBN: 978-3-642-53777-6